THE JOURNAL OF PHYSICAL CHEMISTRY Letters

Letter

pubs.acs.org/JPCL

Liquid Crystallinity and Dimensions of Surfactant-Stabilized Sheets of Reduced Graphene Oxide

Camilo Zamora-Ledezma,[†,‡] Nicolas Puech,[†] Cécile Zakri,[†] Eric Grelet,[†] Simon E. Moulton,[§] Gordon G. Wallace,[§] Sanjeev Gambhir,[§] Christophe Blanc,[∥] Eric Anglaret,[∥] and Philippe Poulin*[,†]

[†]Centre de Recherche Paul-Pascal, Université de Bordeaux - CNRS, 115 Avenue Schweitzer, 33600 Pessac, France

[‡]Laboratorio de Física de la Materia Condensada, Centro de Física, Instituto Venezolano de Investigaciones Científicas, Altos de Pipe, 1204 Caracas, Venezuela

[§]ARC Centre of Excellence for Electromaterials Science, Intelligent Polymer Research Institute, University of Wollongong, New South Wales, Australia

[∥]Laboratoire Charles Coulomb UMR 5221, Université Montpellier II, place Eugène Bataillon, 34095 Montpellier Cedex 5, France

ABSTRACT: Graphene oxide (GO) flakes dissolved in water can spontaneously form liquid crystals. Liquid crystallinity presents an opportunity to process graphene materials into macroscopic assemblies with long-range ordering, but most graphene electronic functionalities are lost in oxidation treatments. Reduction of GO allows recovering functionalities and makes reduced graphene oxide (RGO) of greater interest. Unfortunately, chemical reduction of GO generally results in the aggregation of the flakes, with no liquid crystallinity observed. We report in the present work liquid crystals made of RGO. The addition of surfactants in appropriate conditions is used to stabilize the RGO flakes against aggregation maintaining their ability to form water-based liquid crystals. Structural and thermodynamical studies allow the dimensions of the flakes to be deduced. It is found that the thickness and diameter of RGO flakes are close to that of neat GO flakes.

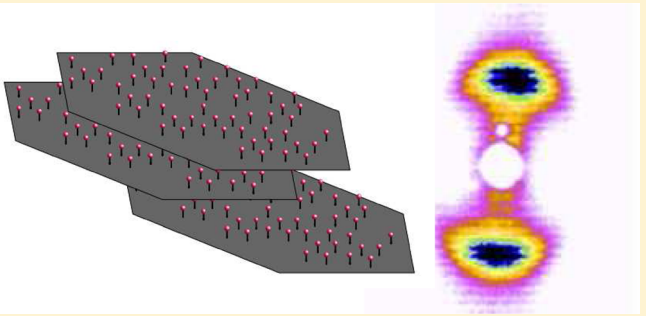

SECTION: Glasses, Colloids, Polymers, and Soft Matter

The use of reduced forms of graphene oxide (GO) flakes allows for easy and scalable production of graphene-based materials potentially useful for various applications[1−4] including nanocomposites,[5,6] paper and membranes,[7] transparent films,[8] and aerogels.[9,10] Optimization of graphene-based materials for most applications necessitates a fine control over the dimensions and level of exfoliation as well as long-range ordering of the reduced graphene oxide (RGO) flakes. Unfortunately, direct imaging techniques such as atomic force miscroscopy (AFM) or electron microscopy are not well-suited for statistical characterizations of the dimensions and exfoliation of graphene. Nevertheless, ordering can be promoted by the spontaneous formation of liquid crystals made of graphene flakes in liquid media. The formation of such liquid crystals requires the stabilization of particles at sufficiently high concentration so that the competition of rotational and translational entropy[11] becomes favorable to the formation of a liquid-crystalline phase. Advances in this field have been recently achieved. Behabtu et al.[12] reported graphene-based liquid crystals in super acids in the absence of moisture. Other groups instead used water-based solutions of GO flakes.[13−16] GO is generally obtained by acid oxidation of graphite materials[17] and is water-soluble, but manipulation of super acids is limiting, and oxidation of graphene is known to downgrade its mechanical and electrical properties severely. Chemical reduction of GO to produce RGO allows a partial restoration of the electronic conjugation and graphene properties, but this recovery is also associated with a gain in hydrophobicity with a loss of water solubility, which hinders liquid-crystal ordering. In addition, reduction of GO flakes after processing in water cannot always be easily achieved. In particular, it can be difficult to perform chemical modifications if fragile electronic devices have been built or if the particles are stacked and not easily accessible for chemical or electrochemical treatments. The direct processing of RGO would in most cases facilitate the use of this material in future applications.

We report an approach that still allows the formation of aqueous lyotropic liquid crystals using RGO despite their lack of water solubility. The objective is to combine the advantages of RGO materials and the easy processing of GO flakes. In this approach, the RGO particles are stabilized by bile salts (BSs), which act as surfactants. Surfactant-stabilized RGO flakes, in contrast with neat RGO, are shown to form liquid crystals in

Received: June 27, 2012
Accepted: August 15, 2012

   dx.doi.org/10.1021/jz3008479 | J. Phys. Chem. Lett. 2012, 3, 2425−2430

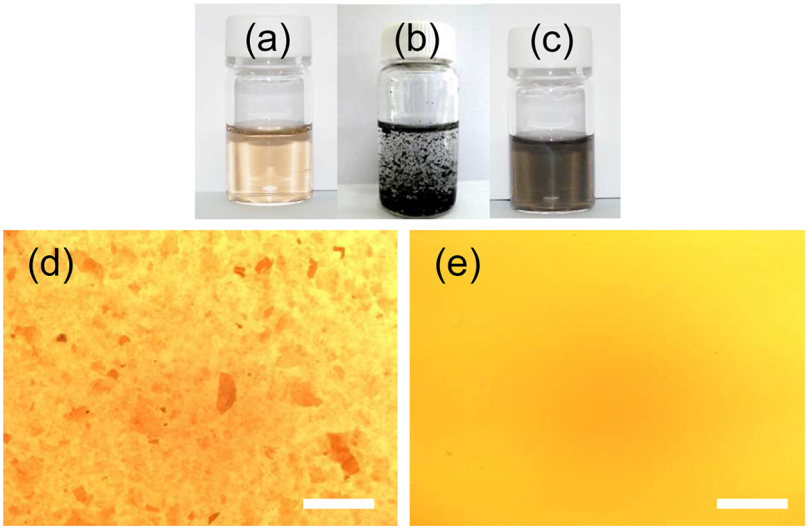

Figure 1. Photographs of vials containing 10 mL of aqueous solutions of (a) graphene oxide (GO), (b) reduced graphene oxide (RGO), and (c) RGO stabilized by bile salts (RGO-BS). The shown solutions contain 0.001 wt % of graphene materials. Pictures are taken a week after each sample preparation. The weight fraction of BS in panel c is 0.5 wt %. Typical brightfield optical micrographs of GO solutions (d) before sonication and (e) after 30 min of tip sonication, followed by a mild centrifugation at 2700*g* during 60 min at room temperature. The uniformity of the picture reveals the absence of particles or aggregates with dimensions that exceed a micrometer, the typical order of the optical microscope resolution. Similar pictures are found for aqueous dispersions of RGO+BS. Scale bar 200 μm.

water. We note that by contrast with GO flakes these particles are metastable colloids. From a thermodynamical point of view, the behavior of surfactant-stabilized RGO is similar to the behavior of surfactant-stabilized colloids or emulsions. The kinetic stabilization is sufficient to achieve dispersions that are stable over months. Such a time scale allows easy processing of graphene-based materials and devices. Further information on the stability of the materials would require observations over longer time scales or analysis of their behavior under osmotic compression, as sometimes performed for colloids and emulsions.

The liquid-crystal phases are observed up to large dilution levels of about 1.0 to 1.5 wt % of RGO. This diluted boundary of the isotropic to liquid-crystal transition is due to the large aspect ratio of the RGO flakes.[18,19] The dilution behavior also shows that van der Waals attractive interactions are efficiently counter-balanced by electrostatic repulsions provided by the surfactants and remaining functional groups at the surface of the RGO flakes. The liquid-crystal structures are characterized by small-angle X-ray scattering (SAXS) experiments that confirm the exfoliation of single-layer graphene flakes. The thickness of GO flakes is found to be of ∼0.5 nm, in good agreement with previous reports on related materials.[15,16,20−22] Moreover, it is found that surfactant-stabilized RGO and GO flakes have approximately the same thickness. This similarity could be ascribed to the presence of surfactant molecules and remaining functional groups at the surface of the RGO particles. The similarities in thickness and phase behavior reveal that GO and RGO sheets have similar lateral dimensions. This reflects the absence of degradation during the chemical reduction. Nevertheless, in contrast with films made of GO, films made of RGO are found to be electrically conductive. This observation confirms the efficiency of the chemical reduction at restoring, even not fully, electronic conjugation and functionalities. From a general point of view, this work also confirms how studies of the liquid crystallinity of graphene materials can provide information on the exfoliation and dimensions of the flakes in bulk. This is valuable information that cannot be easily obtained by direct imaging methods and which is critical to develop applications, materials standardization, and comparisons.

Homogeneity and stability of the solutions were initially assessed by direct observation. A photograph of a vial containing 10 mL of a GO solution at 0.001 wt % is shown in Figure 1a. The typical yellow-brown color of GO solutions is observed. The solution is homogeneous and stable over several months. By contrast, as shown in Figure 1b, a dispersion of RGO flakes in the absence of BS is unstable. The flakes form large black aggregates that quickly sediment. However, as shown in Figure 1c, the flakes can be stabilized against aggregation and sedimentation by the addition of BS surfactant. Similar to neat GO flakes in water, the RGO-BS flakes are stable over several months. Optical microscopy is used to check the solution on a microscopic scale. Typical optical micrographs of GO solutions before and after sonication are, respectively, shown in Figure 1d,e. These optical micrographs reveal the efficiency of sonication at exfoliating and dispersing GO. Indeed, the uniformity of the picture in Figure 1e reflects the absence of particles or aggregates with dimensions that exceed ∼1 μm, the typical order of the optical microscopy resolution. Similar pictures are found for aqueous dispersions of RGO stabilized with BS.

Optical absorbance measurements of GO and RGO flakes are shown in Figure 2a. A typical red shift of the peak located at low wavelengths is observed from 270 nm for RGO to 245 nm for GO. This observation reflects the (partial) restoration of electronic conjugation in RGO.[23] The chemical GO conversion of graphene is assessed by Raman spectroscopy. Typical Raman spectra of raw EG, GO, and RGO-BS are shown in Figure 2b. The graphene weight concentration in both suspensions is 0.001 wt %, and for the RGO-BS suspension, the BS concentration is ∼0.5 wt %.

Several typical features of graphene such as D, G, and G′ bands located around 1358, 1587, and 2720 cm^{-1} are seen in the spectra. The main signatures of the chemical conversions from EG flakes to GO and RGO-BS are a red shift of the G

dx.doi.org/10.1021/jz3008479 | *J. Phys. Chem. Lett.* 2012, 3, 2425−2430

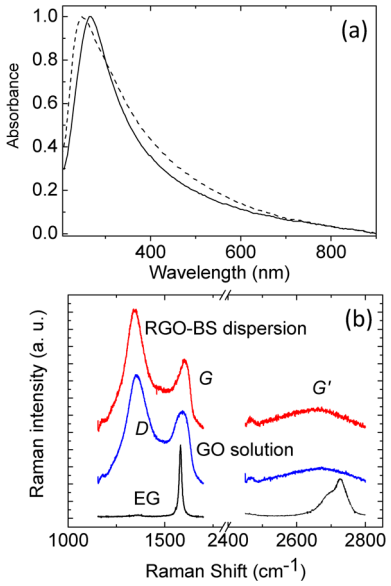

Figure 2. (a) Normalized absorbance spectra of aqueous suspensions of GO (dashed line) and RGO in presence of BS (continuous line). (b) Raman spectra for raw expanded graphite (EG) (bottom), aqueous suspension of GO (middle), and RGO in presence of BS (top). All spectra are normalized by the intensity of the *G* band and shifted along the ordinate axis for clarity. The graphene weight fraction in both suspensions is 0.001 wt %, and for the RGO-BS suspension, the BS concentration is 0.5 wt %.

band, a strong broadening of the three bands, as well as a dramatic increase in the I_D/I_G ratio. This ratio has been determined after baseline subtraction. All of these features, as well as the increase in the I_D/I_G ratio, from 1.35 to 1.51 between GO and RGO-BS, are in good agreement with previous studies,[23,24] which confirms the strong chemical modifications by the oxidative treatments. The final Raman signature of RGO-BS reflects that the reduction does not lead to a full restoration of the EG structure.

The liquid crystallinity of the materials is first assessed by optical microscopy using crossed polarizers. As shown in Figure 3b,d, birefringence and typical nematic textures are observed for concentrated GO and RGO-BS materials. Those nematics are not aligned on a macroscopic scale and exhibit only small disoriented monodomains. The graphene concentrations for these samples are 6.6 and 5.9 wt %, respectively. As expected, the diluted system shown in Figures 1a and 3a does not exhibit such a structure in between crossed polarizers. The RGO suspension in the absence of BS was found to be unstable. This is confirmed in the optical micrograph of Figure 3c with the observation of compact aggregates. This material does not exhibit any phase transition toward a liquid-crystalline state. The BS surfactant plays a critical role because it stabilizes the RGO flakes against their aggregation, allowing thereby liquid-crystal self-ordering. The dispersions form a single nematic phase above a weight fraction of ∼1.5 wt % for both GO and RGO-BS materials. A biphasic region is observed approximately between 1.0 and 1.5 wt %. The materials form a single isotropic phase at lower weight fractions. Assuming a material density of 1.8 g/cm^3,[25] a weight fraction of 1.0 wt % corresponds to a volume fraction of ∼0.6% for the cloud point of the nematic phase. According to theoretical predictions,[18,19] the isotropic−nematic transition for thin platelets is expected at a volume fraction of $\sim 4\ \delta/D$, where δ is the layer thickness and D the diameter of the platelets. We note that this value is an approximate for monodisperse platelets. For monodisperse systems, the width of the biphasic region is relatively narrow.[18,19] Even if this width is not accurately determined in the present work, it seems to be greater than that expected for monodisperse platelets. This phenomenon can presumably be ascribed to the polydispersity of the GO and RGO flakes. Nevertheless, assuming a monodisperse distribution, it is possible to deduce from the above theoretical expectations that the aspect ratios δ/D of GO and RGO particles are similar and of $\sim 1.5 \times 10^{-3}$. The aqueous nematic phases based on GO and RGO are further investigated by SAXS. A series of samples with different weight fractions of graphene materials is prepared

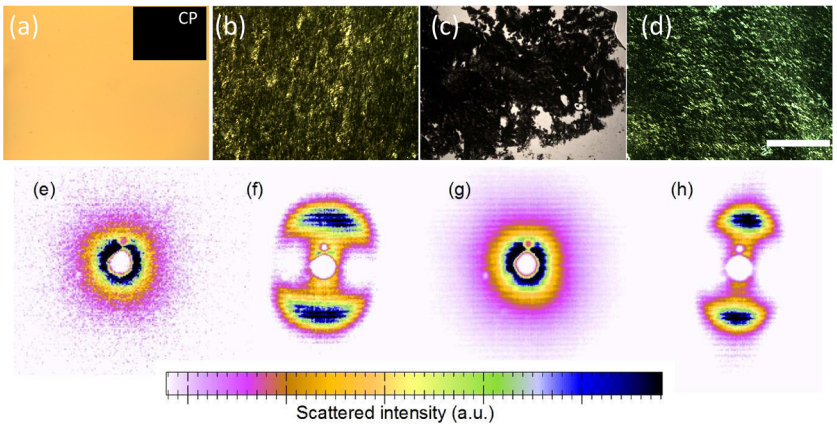

Figure 3. (a) Optical micrograph of an isotropic suspension of diluted GO. The inset shows the same sample observed in between crossed polarizers. (b,d) Optical micrographs between crossed polarizers for concentrated GO (b) and RGO-BS (d) suspensions after a single ultracentrifugation at 210 000*g* during 60 min. The axes of the crossed polarizers are in horizontal and vertical directions for all of the following micrographs: inset of panels a, b, and d. (c) RGO in the absence of BS surfactant: The particles are unstable and form aggregates. The scale bar shown in panel d is 400 μm and is the same for all of the pictures. (e−h) Corresponding SAXS 2D patterns for all graphene aqueous suspensions shown in the first row. The graphene concentrations calculated from absorbance measurements are from left to right: 0.1, 6.6, 5, and 5.9 wt %. The materials in panels f and h exhibit "butterflies" patterns arising from nematic ordering. The patterns are slightly shifted with respect to the horizontal axis. This observation reflects a macroscopic alignment of the director with a small tilt with respect to the capillary tube.

dx.doi.org/10.1021/jz3008479 | J. Phys. Chem. Lett. 2012, 3, 2425−2430

by diluting the samples obtained after ultracentrifugation. Typical 2D diffraction patterns are shown in Figure 3e−h. As expected for the isotropic suspension, the pattern in Figure 3e reflects the absence of pronounced structural ordering. As shown in Figure 3g, a similar result is found for the concentrated RGO suspension in the absence of BS. By contrast the scattered intensities in Figure 3f,h of the GO and RGO-BS stable dispersions exhibit typical "butterflies" anisotropic patterns. The large radial width of this anisotropic pattern reflects a liquid-like order, typical of a nematic organization. It also surprisingly reflects a macroscopic alignment of the director field of the nematic phases with a small tilt with respect to the capillary axis. This macroscopic ordering is ascribed to the shear-induced alignment during centrifugation to fill the capillaries. By contrast, samples observed by optical microscopy are not centrifuged and exhibit a polydomain structure. The alignment of the centrifuged samples is not likely due to centrifugal forces that are very weak in this case. Nevertheless, the present behavior suggests that graphene and GO liquid crystals can be easily aligned despite the large size and aspect ratio of the flakes.

The radial width of the integrated scattered intensity I multiplied by the square of the wave vector q as a function of q is shown in Figure 4a,b for the GO and RGO-BS liquid crystals at different concentrations. The multiplication by q^2 should yield a flat baseline if the scatterers have a plate-like structure.

Peaks at q^* arising from the diffraction of the ordered flakes are clearly observed. These peaks reflect the uniformity of the spacing between the flakes. As shown further, it also confirms single-layer exfoliation of the GO or RGO flakes. The present nematics are made of highly polydisperse disk-like molecules. By contrast with conventional columnar liquid crystals made of monodisperse disks, the present materials can be more likely described as a lamellar structure.[15] This is supported by the observation of peaks at q^* and $2q^*$ in the spectra of some samples for the first- and second-order diffraction peaks. The quasi-flat baseline shows that the form factor of the particles scales as q^{-2}. This dependence confirms the 2D geometry of the scatterers, which are here GO or RGO planes. The distance between stacked neighboring particles, corresponding to a pseudosmectic period, can be directly deduced from the present SAXS measurements. This distance is given by $d = 2\pi/q^*$ and is related to the thickness δ of the layer by the following relationship $d = \delta/\phi$, where ϕ is the material volume fraction. This linear relationship holds only if flakes repel each other so that they fill the whole volume of the sample. If this condition is satisfied, then measurements of q^* as a function of ϕ allow the determination of δ. A linear dependence of d versus $1/\phi$ is actually observed in Figure 4c for both GO and RGO-BS. ϕ was deduced from the known weight fractions of the flakes and assuming a density of 1.8 g/cm^3 for the materials.[24] The present dilution behavior confirms the efficiency of BS at stabilizing flakes of RGO. It is deduced from the slopes of linear fits in Figure 4c that the thicknesses of GO and RGO-BS layers are, respectively, 0.55 and 0.60 nm. These results are in good agreement with previous measurements of the thickness of GO materials,[15,16,19−21] confirming thereby single-layer exfoliation in bulk. In addition, the results provide the first measurements, to our knowledge, of the thickness of RGO flakes stabilized by surfactants. If the materials would be composed of a few layers particles with a distribution of thicknesses, then it would not form liquid crystals with a regular spacing, as evidenced by SAXS. Further analysis by atomic force microscopy or

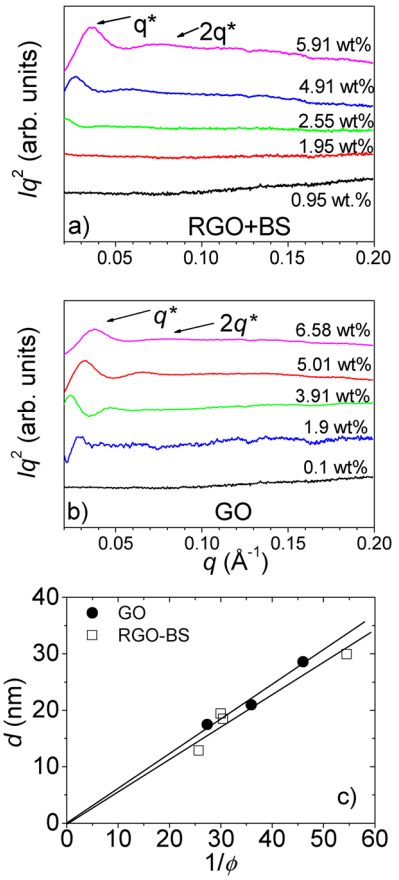

Figure 4. SAXS spectra depicting the scattered intensity as a function of the scattering wave vector q for suspensions of (a) RGO+BS and (b) GO at different concentrations represented by different colors. (c) Characteristic distance $d = 2\pi/q^*$ of the different GO and RGO-BS nematic phases as a function of their inverse volume fraction $(1/\phi)$. Continuous lines are linear fits.

transmission electron microscopy could be useful to obtain pictures of individual flakes but could not provide bulk characterizations. The present observation of thick RGO is explained by considering remaining functional groups and surfactant molecules at the surface of RGO flakes. These similarities reveal that the GO and RGO have similar lateral dimensions (assuming a circular shape for the flakes), confirming thereby the absence of chemical degradation during the chemical reduction. The average diameter D is estimated from the combined thickness ∼0.6 nm deduced from SAXS experiments divided by the aspect ratio $\sim 1.5 \times 10^{-3}$ deduced from the phase behavior. This approach yields $D \approx 400$ nm. This value differs from the value estimated in ref 13 presumably because the raw graphite source was different. The observed differences can also be due to different processing during both functionalization and dispersion. Nevertheless, despite their similar structural and phase behavior, GO and RGO exhibit very different properties. A remarkable difference can be evidenced by investigating dry films made of GO or RGO-BS liquid crystals. GO films made according to the method described in the Experimental Section exhibit a surface resistivity of 500 ± 100 MΩ/sq. Similar films made from RGO-BS liquid crystals exhibit a surface resistivity of 0.7 ± 0.2 MΩ/sq, which differs by almost four orders of magnitude when compared with GO material. These properties will generate significant interest in the use of RGO-BS liquid crystals for

dx.doi.org/10.1021/jz3008479 | J. Phys. Chem. Lett. 2012, 3, 2425−2430

potential applications in electronics, sensors, electrodes, conductive coatings, and so on.

This letter reported the synthesis of water-based liquid crystals composed of reduced GO flakes. The particles were efficiently stabilized at high concentration by BSs molecules. The stability at high concentration leads to the spontaneous formation of nematic phases. More conventional nematic phases made from GO in water were used as reference materials for comparison. Phase behavior and SAXS experiments of samples at different concentrations allowed the dimensions of the graphene sheets to be measured. It was found that neat GO and surfactant-stabilized RGO flakes exhibit comparable thickness and diameter. Despite this apparent structural similarity, GO and RGO exhibit markedly different properties, especially in electrical conductivity. Liquid crystals formed with RGO offer therefore opportunities to develop new materials that combine the advantages of liquid crystallinity for processing and ordering with the richer transport properties of RGO compared with GO. We stress that the same concept of surfactant stabilization may be efficient for the stabilization of large aromatic macromolecules. Dissolution of such molecules remains indeed a great challenge, and their combination with surfactants may lead to novel forms of hybrid liquid crystals. Further research could also be devoted to reduced and chemically doped graphene, which exhibit improved electronic properties.[29,30] From a more general point of view, this work shows how studies of graphene materials in liquid-crystalline states can provide information on the average dimensions of the flakes. Such information cannot be easily achieved via other approaches such as direct imaging by AFM or TEM but are of critical importance to develop future applications and materials standardization.

■ EXPERIMENTAL SECTION

Expanded graphite (EG) from Nacional de Grafite, Minas Gerais, Brazil, is used as the source material. GO is obtained by following the so-called modified Hummers method,[17,22] which involves two oxidation stages. In a typical procedure, the first oxidation is achieved in the following conditions: 1100 mg of EG is placed in a 1000 mL boiling flask. Then, 20 g of $K_2S_2O_8$, 20 g of P_2O_5, and 400 mL of a concentrated aqueous solution of H_2SO_4 (96%) are added in the flask. The mixture is heated under reflux during 6 h and then let at rest during 20 h at room temperature. Oxidized graphite is filtered and rinsed with abundant distilled water until neutral pH. A wet cake-like material is recovered at the end of this first oxidation. For the second oxidation process, the previously collected wet cake is placed in a boiling flask that contains 69 mL of a concentrated aqueous solution of H_2SO_4 (96%). The flask is kept in an ice bath as 9 g of $KMnO_4$ is slowly added. Care is taken to avoid overheating. The resulting mixture is stirred at 35 °C for 2 h, and the sample color turns dark green, followed by the addition of 140 mL of water. After 15 min, the reaction is completed by adding 420 mL of water and 15 mL of an aqueous solution of 30 wt % H_2O_2. The color of the sample at this stage turns bright yellow. To remove the metallic ions, the mixture is filtered and rinsed with a 1:10 HCl aqueous solution. The collected material is gently centrifuged at 2700*g* and rinsed with deionized water. The final product is a wet cake that contains 1.4 wt % of GO, as estimated from dry extracts. Oxidation is expected to yield thermodynamically stable solution of GO flakes. Nevertheless, it can take a long time for this stable state to be reached. This is why liquid dispersions of GO flakes are obtained by sonicating wet-cake materials, which are diluted in deionized water. Sonication is used in the present work to more quickly achieve homogeneous solutions.

Surfactant-stabilized RGO (RGO-BS) is achieved by diluting the wet-cake in an aqueous solution of BSs instead of pure water. A commercially available mixture of cholate sodium (50 wt %) and deoxycholate sodium (50 wt %) salts provided by Sigma Aldrich is used. BS surfactants have been chosen because they were found to be particularly efficient at stabilizing carbon nanotubes in water,[26] including highly ordered carbon-nanotube liquid crystals.[27,28] The BS weight fraction is 0.5 wt %. This fraction is kept constant for all samples. In all of the following steps, surfactant-stabilized systems of RGO are achieved by using aqueous solutions of BSs instead of pure water. Sonication is performed using a Branson Sonifier S-250A equipped with a 13 mm step disruptor horn and a 3 mm tapered microtip, operating at a 20 kHz frequency. Typically, 10 mL of aqueous solutions containing 0.1 wt % of GO is sonicated during 30 min and subsequently centrifugated at 2700*g* during 30 min to remove any nondissolved large particles, aggregates, and impurities. Chemical reduction of as-obtained GO to yield RGO is done by following a method already reported in ref 3. Typically 10 mL of a 0.1 wt % GO aqueous solution is placed in a boiling flask of 50 mL. We add 10 μL of a 35 wt % aqueous solution of N_2H_4 (hydrazine) and 70 mL of a 28 wt % of an aqueous solution of NH_4OH (ammonia) to the mixture, which is stabilized by BS. The solution is homogenized and heated to 90 °C under stirring and reflux during 1 h. The pH measured after the reaction is ∼11. The color of the sample turns dark black during the reduction reaction.

The above suspensions (GO in water and RGO in BS/water) are subjected to a single ultracentrifugation at 210 000*g* for 60 min to obtain lyotropic liquid-crystal phases. Concentrated sediments are obtained at the bottom of the vials. The weight fraction of the flakes in the concentrated sediment is measured by optical absorbance at a wavelength of 400 nm. Calibration curves for such experiments have been previously determined using solutions of GO and RGO of known weight fractions. Weight fractions in these reference solutions were deduced from gravimetric extracts. Concentrated phases are then rediluted with pure water or with aqueous solutions of BS to vary and control the volume fraction of the flakes.

The obtained samples are characterized by optical microscopy, Raman spectroscopy, and small-angle X-ray scattering. Raman measurements are performed using the green laser line (514 nm) from an Ar laser as excitation source and a Jobin-Yvon T64000 spectrometer operating in a single grating (1800 gr/mm) configuration. For X-ray measurements, cylindrical quartz capillary tubes of 0.5 mm in diameter are filled with isotropic dispersions and nematic phases. The capillaries are centrifuged at 2700*g* during 1 min to let the viscous sample settle at the bottom of the tubes. SAXS experiments are performed on a Brüker Nanostar instrument, which operates at a wavelength of 1.54 Å and which is equipped with a vacuum chamber in which the capillaries are inserted. The scattering wave-vector ranges from 0.01 to 0.2 $Å^{-1}$.

Conductive thin films made from nematic liquid crystals of GO and RGO-BS are obtained by depositing a drop of nematic suspension onto a glass substrate and shearing it in a single direction with a second glass slide on top of it. Therefore, macroscopic areas of about 2 × 3 cm^2 are covered by oriented graphene liquid crystals. The upper slide is removed so that

dx.doi.org/10.1021/jz3008479 | J. Phys. Chem. Lett. 2012, 3, 2425−2430

water evaporates to achieve dried and oriented dried thin films. The thickness of the films is ~200 nm, as determined with a mechanical profilometer and by atomic force microscopy. Then, small areas of 5 × 5 mm^2 square are isolated, and two of the edges are subsequently coated with silver paste, which serves as electrodes for surface conductivity measurements. Two-probe conductivity measurements were carried out at room temperature using a Keithley 2000 multimeter. All samples were kept at 80 °C under vacuum during 24 h prior each measurement to avoid artifacts due to the presence of moisture.

AUTHOR INFORMATION

Notes

The authors declare no competing financial interest.

ACKNOWLEDGMENTS

We thank the European Commission for financial support of this work in the frame of the COMPLOIDS project.

REFERENCES

(1) Geim, A. K.; Novoselov, K. S. The Rise of Graphene. *Nat. Mater.* **2007**, *6*, 183−191.
(2) Geim, A. K. Graphene: Status and Prospects. *Science* **2009**, *324*, 1530−1534.
(3) Li, D.; Muller, M. B.; Gilje, S.; Kaner, R. B.; Wallace, G. G. Processable Aqueous Dispersions of Graphene Nanosheets. *Nat. Nanotechnol.* **2008**, *3*, 101−105.
(4) Stankovich, S.; Dikin, D. A.; Piner, R. D.; Kohlhaas, K. A.; Kleinhammes, A.; Jia, Y.; Wu, Y.; Nguyen, S. T.; Ruoff, R. S. Synthesis of Graphene-Based Nanosheets via Chemical Reduction of Exfoliated Graphite Oxide. *Carbon* **2007**, *45*, 1558−1565.
(5) Stankovich, S.; Dikin, D. A.; Dommett, G. H. B.; Kohlhaas, M. K.; Zimney, E. J.; Stach, E. A.; Piner, R. D.; Nguyen, S. T.; Ruoff, R. S. Graphene-Based Composite Materials. *Nature* **2006**, *442*, 282−286.
(6) Ramanathan, T.; Abdala, A. A.; Stankovich, S.; Dikin, D. A.; Herrera-Alonso, M.; Piner, R. D.; Adamson, D. H.; Schniepp, H. C.; Chen, X.; Ruoff, R. S.; et al. Functionalized Graphene Sheets for Polymer Nanocomposites. *Nat. Nanotechnol.* **2008**, *3*, 327−331.
(7) Chen, H.; Muller, M. B.; Gilmore, K. J.; Wallace, G. G.; Li, D. Mechanically Strong, Electrically Conductive, And Biocompatible Graphene Paper. *Adv. Mater.* **2008**, *20*, 3557−3561.
(8) Yu, A.; Roes, I.; Davies, A.; Chen, Z. Ultrathin, Transparent, And Flexible Graphene Films for Supercapacitor Application. *Appl. Phys. Lett.* **2010**, *96*, 253105.
(9) Worsley, M. A.; Pauzauskie, P. J.; Olson, T. Y.; Biener, J.; Satcher, J. H.; Baumann, T. F. Synthesis of Graphene Aerogel with High Electrical Conductivity. *J. Am. Chem. Soc.* **2010**, *132*, 14067−14069.
(10) Zhang, X.; Sui., Z.; Xu., B.; Yue., S.; Luo., Y.; Zhan., W.; Liu, B. Mechanically Strong and Highly Conductive Graphene Aerogel and Its Use As Electrodes for Electrochemical Power Sources. *J. Mater. Chem.* **2011**, *21*, 6494−6497.
(11) Onsager, L. The Effects of Shape on the Interaction of Colloidal Particles. *Ann. N.Y. Acad. Sci.* **1949**, *51*, 627−659.
(12) Behabtu, N.; Lomeda, J. R.; Green, M. J.; Higginbotham, A. L.; Sinitskii, A.; Kosynkin, D. V.; Tsentalovich, D.; Parra-Vasquez, A. N.G.; Schmidt, J.; Kesselman, E.; et al. Spontaneous High-Concentration Dispersions and Liquid Crystals of Graphene. *Nat. Nanotechnol.* **2010**, *5*, 406−411.
(13) Dan, B.; Behabtu, N.; Martinez, A.; Evans, J. S.; Kosynkin, D. V.; Tour, J. M.; Pasquali, M.; Smalyukh, I. I. Liquid Crystals of Aqueous, Giant Graphene Oxide Flakes. *Soft Matter* **2011**, *7*, 11154−11159.
(14) Kim, J. E.; Han, T. H.; Lee, S. H.; Kim, J. Y.; Ahn, C. W.; Yun, J. M.; Kim, S. O. Graphene Oxide Liquid Crystals. *Angew. Chem., Int. Ed.* **2011**, *50*, 3043−3047.
(15) Xu, Z.; Gao, C. Aqueous Liquid Crystals of Graphene Oxide. *ACS Nano* **2011**, *5*, 2908−2915.
(16) Gudarzi, M. M.; Zheng, Q. B.; Kim, J.-K. Spontaneous Formation of Liquid Crystals in Ultralarge Graphene Oxide Dispersions. *Adv. Funct. Mater.* **2011**, *21*, 2978−2988.
(17) Hummers, W.; Offeman, R. Preparation of Graphitic Oxide. *J. Am. Chem. Soc.* **1958**, 1339−1339.
(18) van der Kooij, F. M.; Lekkerkerker, H. N. W. Formation of Nematic Liquid Crystals in Suspensions of Hard Colloidal Platelets. *J. Phys. Chem. B* **1998**, *102*, 7829−7832.
(19) Veerman, J. A. C.; Frenkel, D. Phase-Behavior of Disk-Like Hard-Core Mesogens. *Phys. Rev. A* **1992**, *45*, 5632−5648.
(20) Hontorialucas, C.; Lopezpeinado, A. J.; Lopezgonzalez, J. D. D.; Rojascervantes, M. L.; Martinaranda, R. M. Study of Oxygen-Containing Groups in a Series of Graphite Oxides - Physical and Chemical Characterization. *Carbon* **1995**, *33*, 1585−1592.
(21) Medhekar, N. V.; Ramasubramaniam, A.; Ruoff, R. S.; Shenoy, V. B. Hydrogen Bond Networks in Graphene Oxide Composite Paper: Structure and Mechanical Properties. *ACS Nano* **2010**, *4*, 2300−2306.
(22) Kovtyukhova, N. I.; Ollivier, P. J.; Martin, B. R.; Mallouk, T. E.; Chizhik, S. A.; Buza15-neva, E. V.; Gorchinskiy, A. D. Layer-by-Layer Assembly of Ultrathin Composite Films from Micron-Sized Graphite Oxide Sheets and Polycations. *Chem. Mater.* **1999**, *11*, 771−778.
(23) Zhou, Y.; Bao, Q.; Tang, L. A. L.; Zhong, Y.; Loh, K. P. Hydrothermal Dehydration for the "Green" Reduction of Exfoliated Graphene Oxide to Graphene and Demonstration of Tunable Optical Limiting Properties. *Chem. Mater.* **2009**, *21*, 2950−2956.
(24) Zhang, W.; He, W.; Jing, X. Preparation of a Stable Graphene Dispersion with High Concentration by Ultrasound. *J. Phys. Chem. B* **2010**, *114*, 10368−10373.
(25) Dikin, D. A.; Stankovich, S.; Zimney, E. J.; Piner, R. D.; Dommett, G. H. B.; Evmenenko, G.; Nguyen, S. T.; Ruoff, R. S. Preparation and Characterization of Graphene Oxide Paper. *Nature* **2007**, *448*, 457−460.
(26) Wenseleers, W.; Vlasov, I. I.; Goovaerts, E.; Obraztsova, E. D.; Lobach, A. S.; Bouwen, A. Efficient Isolation and Solubilization of Pristine Single-Walled Nanotubes in Bile Salt Micelles. *Adv. Funct. Mater.* **2004**, *14*, 1105−1112.
(27) Puech, N.; Blanc, C.; Grelet, E.; Zamora-Ledezma, C.; Maugey, M.; Zakri, C.; Anglaret, E.; Poulin, P. Highly Ordered Carbon Nanotube Nematic Liquid Crystals. *J. Phys. Chem. C* **2011**, *115*, 3272−3278.
(28) Puech, N.; Grelet, E.; Poulin, P.; Blanc, C.; van der Schoot, P. Nematic Droplets in Aqueous Dispersions of Carbon Nanotubes. *Phys. Rev. E* **2010**, *82*, 020702.
(29) Hwang, J. O.; Park, J. S.; Choi, D. S.; Kim, J. Y.; Lee, S. H.; Lee, K. E.; Kim, Y. H.; Song, M. H.; Yoo, S.; Kim, S. O. Workfunction-Tunable, N-Doped Reduced Graphene Transparent Electrodes for High-Performance Polymer Light-Emitting Diodes. *ACS Nano* **2012**, *6*, 159−167.
(30) Park, S.; Hu, Y.; Hwang, J. O.; Lee, E.-S.; Casabianca, L. B.; Cai, W.; Potts, J. R.; Ha, H.-W.; Chen, S.; Oh, J.; Kim.; et al. Chemical Structures of Hydrazine-Treated Graphene Oxide and Generation of Aromatic Nitrogen Doping. *Nat. Commun.* **2012**, *3*, 638.